JOURNAL OF GEOPHYSICAL RESEARCH, VOL. 114, D17107, doi:10.1029/2009JD012105, 2009

An observationally based energy balance for the Earth since 1950

D. M. Murphy,[1] S. Solomon,[1] R. W. Portmann,[1] K. H. Rosenlof,[1] P. M. Forster,[2] and T. Wong[3]

Received 20 March 2009; revised 3 June 2009; accepted 18 June 2009; published 9 September 2009.

[1] We examine the Earth's energy balance since 1950, identifying results that can be obtained without using global climate models. Important terms that can be constrained using only measurements and radiative transfer models are ocean heat content, radiative forcing by long-lived trace gases, and radiative forcing from volcanic eruptions. We explicitly consider the emission of energy by a warming Earth by using correlations between surface temperature and satellite radiant flux data and show that this term is already quite significant. About 20% of the integrated positive forcing by greenhouse gases and solar radiation since 1950 has been radiated to space. Only about 10% of the positive forcing (about 1/3 of the net forcing) has gone into heating the Earth, almost all into the oceans. About 20% of the positive forcing has been balanced by volcanic aerosols, and the remaining 50% is mainly attributable to tropospheric aerosols. After accounting for the measured terms, the residual forcing between 1970 and 2000 due to direct and indirect forcing by aerosols as well as semidirect forcing from greenhouse gases and any unknown mechanism can be estimated as -1.1 ± 0.4 W m^{-2} (1σ). This is consistent with the Intergovernmental Panel on Climate Change's best estimates but rules out very large negative forcings from aerosol indirect effects. Further, the data imply an increase from the 1950s to the 1980s followed by constant or slightly declining aerosol forcing into the 1990s, consistent with estimates of trends in global sulfate emissions. An apparent increase in residual forcing in the late 1990s is discussed.

Citation: Murphy, D. M., S. Solomon, R. W. Portmann, K. H. Rosenlof, P. M. Forster, and T. Wong (2009), An observationally based energy balance for the Earth since 1950, *J. Geophys. Res.*, *114*, D17107, doi:10.1029/2009JD012105.

1. Introduction

[2] Conservation of energy is a powerful tool for analyzing physical systems. The Earth's climate system is no exception. Net positive climate forcing causes the Earth to retain energy that is primarily stored in the oceans. Although there may be variability in individual terms, the requirement for energy conservation has no natural cycles.

[3] An important feature of the Earth's energy budget is that the amount of infrared radiation leaving the Earth is determined by locations (the surface and atmosphere) with much smaller heat capacities than the ocean beneath the surface layer. This leads to multiple time scales in the response to a climate forcing. Two prominent time scales in the response to a climate perturbation are a partial surface temperature response in about 10 years and an ocean response of centuries [*Stouffer*, 2004; *Knutti et al.*, 2008].

[4] The differing time scales imply that ocean heat content and surface temperature contain distinct information about the Earth's response to radiative forcing [*Gregory*, 2000]. Over a time scale of decades, the ocean is heated by the integral of the radiative imbalance of the surface and atmosphere. A faster land and ocean surface temperature response to a given forcing will actually slow the rate of increase in the overall ocean heat content because the increased outgoing radiation from a warmer surface means that there is less energy available to heat the ocean. Figure 1 is a schematic diagram of the energy available to heat the Earth after an idealized step function change in radiative forcing.

[5] Energy flows in the climate system have been studied previously, especially seasonal cycles [*Trenberth and Stepaniak*, 2004; *Tsushima et al.*, 2005; *Fasullo and Trenberth*, 2008]. Average global heat fluxes were described by *Trenberth et al.* [2009]. Several authors have shown that global climate models can explain the main features of ocean heat uptake if they include the effects of recent large volcanic eruptions [*Levitus et al.*, 2001; *Barnett et al.*, 2005; *Church et al.*, 2005; *Delworth et al.*, 2005; *Hansen et al.*, 2005; *Domingues et al.*, 2008]. The Earth's heat budget has also been used to put limits on the climate sensitivity using global climate models [e.g., *Knutti et al.*, 2002; *Stott et al.*, 2008] and data [*Gregory et al.*, 2002].

[6] Our approach in this paper is to examine the limits that can be placed on the Earth's energy budget not by using climate models but rather based strictly on observations: we use measurements of surface temperature, ocean heat content and satellite observations of radiative fluxes. We also use published results from radiative transfer calculations of

[1]Chemical Sciences Division, Earth System Research Laboratory, NOAA, Boulder, Colorado, USA.
[2]School of Earth and Environment, University of Leeds, Leeds, UK.
[3]NASA Langley Research Center, Hampton, Virginia, USA.

0148-0227/09/2009JD012105$09.00

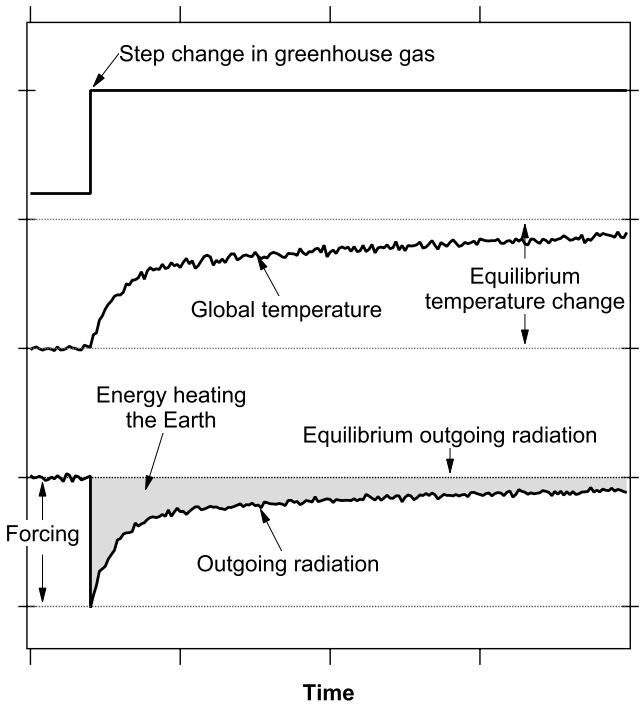

Figure 1. Illustrative sketch of the response of the Earth energy budget to an idealized step function change in a greenhouse gas. Outgoing radiation from the Earth at first decreases then returns toward an equilibrium value as the Earth warms. An initial rapid temperature response, as plotted here, reduces the amount of energy available to heat the Earth and slows the eventual approach to equilibrium.

the forcing due to greenhouse gases and volcanic aerosols as well as the sun. The remaining energy is primarily due to the direct and indirect radiative effects of aerosols. Any semidirect forcing due to greenhouse gases [*Andrews and Forster*, 2008] and any other unresolved forcings are also included in the residual. The change in the energy budget due to aerosols is left as the residual between these observed terms largely because of the uncertainty in their indirect effects on clouds. Although some estimates have been made from satellite data over limited periods, these are subject to large uncertainties and are not available over the multi-decadal timescales of interest here.

2. Data Sources for Heat Content and Radiative Forcing

2.1. Ocean, Land, and Atmospheric Heat Content

[7] There are several recent calculations of observed ocean heat contents from the surface to 700 m depth [*Domingues et al.*, 2008; *Ishii and Kimoto*, 2009; *Levitus et al.*, 2009]. In each study, temperature profiles were converted to estimates of the ocean heat content. Each study also corrects expendable bathy-thermograph (XBT) measurements using fall rate or empirical corrections. These corrections make the heat content estimates more accurate than previous estimates using similar data [*Wijffels et al.*, 2008].

[8] In addition to heating of the top 700 m, some heat is transported to the deep ocean. The heat content to 3000 m depth has been estimated to add about 30% to 40% to recent increases above 700 m on the basis of limited deep ocean temperature data [*Levitus et al.*, 2001]. Another estimate [*Köhl et al.*, 2007] based on an ocean model assimilation of temperature, wind stress, and other data leads to a 40% correction for heat transported deeper than 700 m, with most of this after 1990 [*Köhl and Stammer*, 2008]. The coefficient of thermal expansion of water varies with temperature and depth, so steric sea level rise does not uniquely constrain ocean heat content. For the purposes of this paper we estimate that from 1950 to 2003 the increase in the heat content of the ocean deeper than 700 m was 40 ± 15% of the increase from 0 to 700 m. For a given year, the deep ocean heat content is scaled to the heat content above 700 m averaged over the preceding 10 years. The actual lag may be longer but the results here are insensitive to the averaging period and longer averages require more assumptions about the heat content before 1950.

[9] Changes in atmospheric, land, and ice heat contents are very small compared to the oceans [*Levitus et al.*, 2005]. The atmospheric heat content since 1950 was computed using the surface temperature record and the heat capacity of the troposphere. Land and ice heat contents were scaled to the previous 4 years of surface temperatures using values in Figure 5.4 of the Intergovernmental Panel on Climate Change (IPCC) Fourth Assessment Report (AR4) [*Bindoff et al.*, 2007].

2.2. Radiative Forcing

[10] Greenhouse gases and volcanic eruptions are both major sources of radiative forcing since 1950. The radiative properties of the major greenhouse gases can be considered to be known to high accuracy on the basis of laboratory studies, line-by-line calculations of radiative transfer, and radiative model intercomparisons [see *Forster et al.*, 2007, and references therein]. We use a time history of radiative forcing from *Gregory and Forster* [2008] with two modifications. Their volcanic forcing is smoothed and the resulting low time resolution is not suitable for the analysis here. We used the stratospheric aerosol forcing from the Goddard Institute for Space Studies (GISS) compilation (http://data.giss.nasa.gov/modelforce/RadF.txt) instead. The *Gregory and Forster* [2008] and GISS stratospheric aerosol forcing are essentially identical except for the smoothing. Second, the *Gregory and Forster* [2008] stratospheric ozone forcing was scaled by a factor of 0.45 to match the AR4 best estimate of -0.05 W m^{-2} [*Forster et al.*, 2007].

[11] Radiative forcing from long-lived trace gases is based on observations of their concentrations along with radiative transfer calculations. The time history used here is very close to the detailed calculations by *Myhre et al.* [2001]. The 1σ uncertainty in forcing from long-lived greenhouse gases is estimated as ±5% on the basis of *Collins et al.* [2006]. Uncertainties of ±30% were assumed for smaller forcings from tropospheric ozone and solar variability. The radiative forcings here do not include any semidirect effects of CO_2 and other greenhouse gases [*Andrews and Forster*, 2008], which will therefore be included in the residual forcing along with aerosol direct and indirect effects.

[12] The stratospheric aerosol radiative forcings for recent decades are ultimately based upon data from the SAGE

instruments and other observations of stratospheric aerosol extinction along with relationships developed by *Lacis et al.* [1992], who used a radiative transfer model and balloon-borne size distribution data to convert measured extinction to radiative forcing. We use ±25% uncertainty after 1980 and double the uncertainty before 1980 because of the lack of satellite data. As will be shown later, the perturbations in ocean heat uptake after the eruptions of Agung, El Chichon and Mt. Pinatubo are in very good agreement with the estimated volcanic forcings.

3. Surface Temperature and Net Radiation

[13] A warming Earth emits more infrared radiation. This is the most important restoring term producing a stable climate. There are also important changes in net radiation caused by temperature-induced changes in water vapor, lapse rate, cloudiness, snow cover, and other feedbacks. Ideally, these terms could be constrained by long-term measurements of the net radiation balance of the Earth. The Earth Radiation Budget Experiment (ERBE) nonscanner wide field of view instrument on the Earth Radiation Budget Satellite [*Wong et al.*, 2006] and the Clouds and the Earth's Radiant Energy System (CERES) scanner instrument on the Terra satellite [*Loeb et al.*, 2009] provide radiative flux measurements at the top of the atmosphere but do not span the entire period from 1950 onward. Because of absolute calibration offsets in these two data sets, we use an approach similar to *Forster and Gregory* [2006] that relies on the excellent year-to-year precision of the ERBE and CERES data. In this method, the net radiation balance of the Earth is parameterized as a linear function of temperature. Then this linear function of temperature is used to estimate changes in net radiation for the entire time period from 1950 to present.

[14] A linearized version of the Earth's energy balance is

$$N = F - \lambda \Delta T + \varepsilon, \tag{1}$$

where N is the net energy flow into the Earth, F is the net forcing, $\lambda\Delta T$ is the change in net radiation due to a temperature change ΔT, and ε is measurement noise and internal variability [*Foster et al.*, 2008; *Forster and Gregory*, 2006]. Over a sufficiently long time period, $1/\lambda$ represents the climate sensitivity: when $\Delta T = F/\lambda$, N goes to zero and the Earth no longer warms. Here we are interested in a somewhat different meaning of λ, as the coefficient that best predicts interannual to decadal changes in net radiation as a function of surface temperature. Values of λ appropriate to century time scales can be different than those appropriate to a few years [*Knutti et al.*, 2008] so the values used in this paper should not be interpreted in terms of equilibrium climate sensitivity. Different types of forcings may also have different values of λ. We assume that a value of λ derived from the periods covered by ERBE and CERES (20 years with gaps) can be applied to a continuous 55-year period. We also assume that the mix of forcings during the satellite years is similar enough to all the decades since 1950 for the value of lambda to remain constant.

[15] Our sign convention is that energy heating the Earth is positive. ERBE and CERES longwave and shortwave fluxes are therefore negative because they represent energy leaving the Earth. We also note that by using measurements of net energy flow N from ERBE and CERES rather than writing $N = c\, dT/dt$ where c is a heat capacity, we avoid the complications about multiple time scales that arise from the choice of heat capacity [*Foster et al.*, 2008].

[16] There are some physical constraints on λ. A stable climate system requires λ to have a long-term average value greater than zero. Considering only blackbody radiation with the Earth's existing emissivity and no climate feedbacks, λ would be about 3.2 W m^{-2} K^{-1} [*Soden and Held*, 2006].

[17] Two previous papers estimated λ from ERBE data and surface temperatures. *Forster and Gregory* [2006] performed regressions for various time periods, averaging methods, and temperature records. A typical value is $\lambda = 2.4 \pm 0.8$ W m^{-2} K^{-1} (1σ) using ERBE annual averages for 1985 through 1990 and GISS temperatures. *Tsushima et al.* [2005] derived $\lambda = 0.98 \pm 0.2$ W m^{-2} K^{-1} from the seasonal variation of temperature and ERBE net radiation data. They consider this to be smaller than the correct value for interannual time periods because seasonal time scales may have excessive snow feedbacks. They estimated a long-term slope appropriate to climate sensitivity of about 1.3 W m^{-2} K^{-1}.

[18] From equation (1), the slope of N-F versus ΔT will yield λ. We performed new regressions using 1985 to 1999 data from the ERBE nonscanner instrument on the ERBS satellite and 2000 to 2005 data from the CERES scanner instrument on the Terra satellite. The ERBE wide field of view data cover 60°S to 60°N latitude. The ERBE data are 72-day averages with this period chosen to minimize temporal sampling errors due to orbital precession. These ERBE_S10N_WFOV_ERBS_Edition3_Rev1 data include corrections for altitude changes of the satellite orbit and for degradation of the shortwave dome [*Wong et al.*, 2006]. Since the longwave data are the difference between broadband and shortwave data, the dome correction influences both the shortwave and longwave values but not the total. The CERES data are monthly averages from version CERES_EBAF_TOA_Terra_Edition1A. Temperatures are from National Centers for Environmental Prediction (NCEP) reanalysis averaged over the same latitudes and times as the satellite data. The forcings F are as described earlier. The satellite data are during a period of relatively constant sulfate emissions and we assume that aerosol forcings are constant enough over short time periods not to affect the analysis. This is justified by the advanced very high resolution radiometer (AVHRR) data discussed below with details in Appendix A.

[19] In Figure 2 we show data including both seasonal and annual changes, then verify the calculation with a method that includes only interannual changes (Appendix A). Including seasonal temperature changes in the regression gives a broader range of temperatures than if annual averages are plotted. The wider temperature range yields much better constraints on a slope versus temperature. The main disadvantage is that changes in cloudiness and other parameters with seasonal temperature changes represent feedbacks on a short time scale and may not be accurate predictors of how those parameters will change for interannual temperature changes of the same magnitude. A minor point is that for shortwave radiation the annual cycle of solar radiation due to the changing Earth-Sun distance as well as slower solar

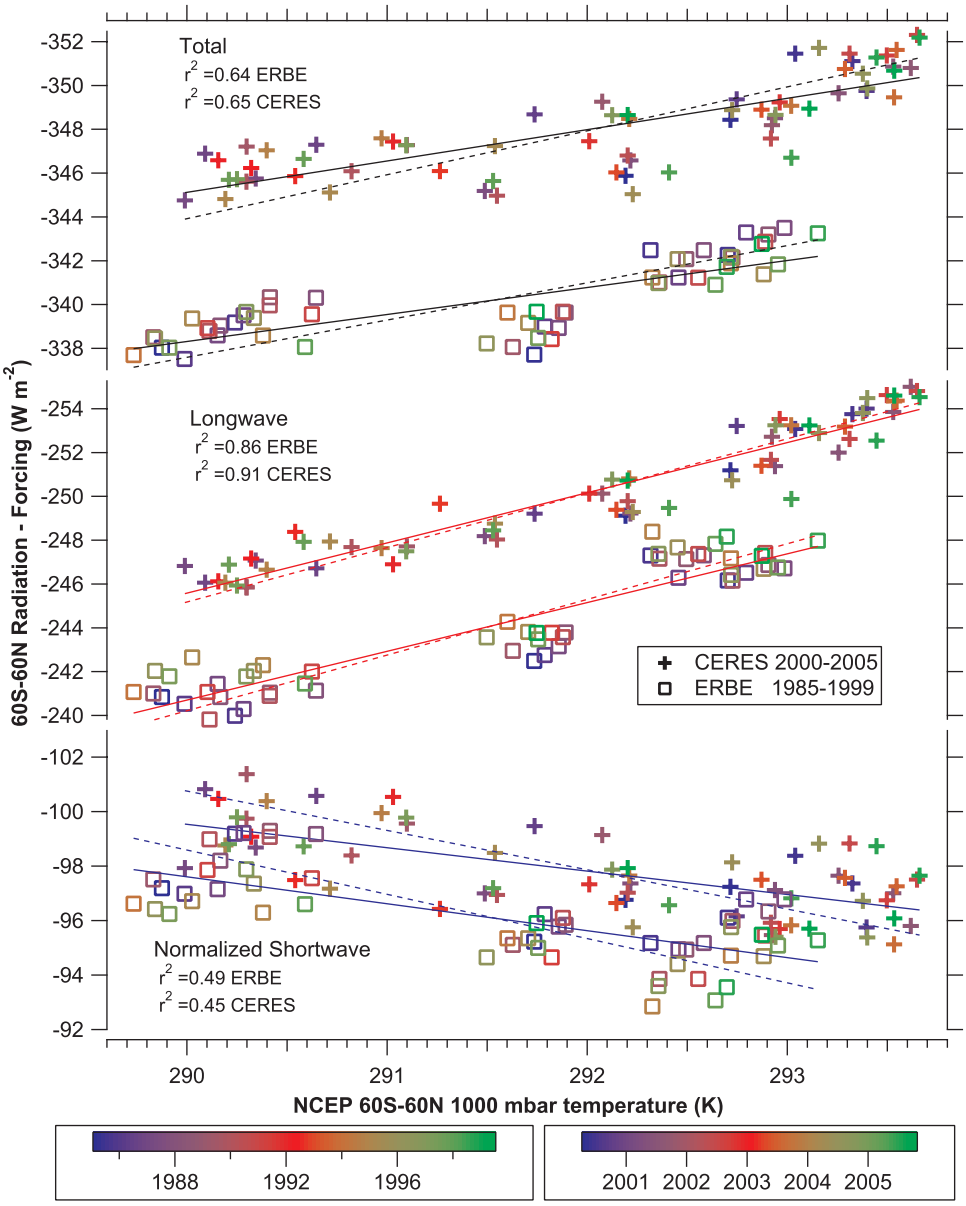

Figure 2. Regressions of ERBE and CERES outgoing radiation minus changes in radiative forcing to give the parameter λ in equation (1). Each ERBE point is one 72-day "season" and each CERES point is 1 month. Temperatures include both interannual and seasonal variations. Solid lines are linear fits using ordinary regression and dashed lines using orthogonal distance regression. Slopes are shown in Table 1; r^2 values are for ordinary regression. Vertical offsets are mostly due to absolute calibration differences and different sampling of the diurnal cycle by the sun-synchronous Terra and nonsynchronous ERBS satellites.

changes must be removed before analysis. This has been done by normalizing the shortwave fluxes to the incident solar radiation (also provided by ERBE and CERES). This amounts to fitting albedo variation, a physical response of the Earth, as opposed to reflected solar radiation, a quantity that varies even if the Earth is unchanged. Note that long-term changes in solar input are included as a forcing.

[20] One question is the proper direction of the regression: whether temperature or outgoing radiation is considered the independent variable for the regression analysis or a neutral regression model is used. We favor ordinary regression of outgoing radiation against temperature for two reasons. First, we use λ to predict net outgoing radiation from observed temperature changes and ordinary regression against temperature matches this use. Second, time response favors regression against temperature on relatively short time scales. If temperature variations are changing outgoing radiation then temperature should be the independent variable whereas if radiation variations are affecting temperature then temperature should be the dependent variable. Although both are true to some extent, they can be partially separated by time response: outgoing radiation changes are mostly immediate whereas surface temperatures lag radiative forcing. Autocorrelation analyses

Table 1. Estimates of the Slope of the Earth Energy Budget Versus Temperature[a]

Source	Method	Source and Time Span	Temperature Record	Longwave[b]	Shortwave[b]	Total[b]
This work	Interannual and seasonal cycle together	ERBE 1985–1999 except 1991.5–1993.5	NCEP 1000 mbar	2.21 ± 0.12, 2.54 ± 0.14	−0.90 ± 0.14, −1.62 ± 0.19	1.31 ± 0.13, 1.71 ± 0.16
This work	Interannual and seasonal cycle together	CERES 2000–2005 (60°S–60°N)	NCEP 1000 mbar	2.29 ± 0.09, 2.48 ± 0.10	−0.86 ± 0.12, −1.44 ± 0.16	1.43 ± 0.13, 2.01 ± 0.17
This work	Interannual and seasonal cycle together	CERES 2000–2005 (global)	NCEP 1000 mbar	2.23 ± 0.07, 2.34 ± 0.07	−1.77 ± 0.21, −3.13 ± 0.35	0.46 ± 0.19, 3.89 ± 1.13
This work	Interannual each season, then average seasons	ERBE 1985–1999 except 1991.5–1993.5	HadCRUT3	2.82 ± 0.42	−1.86 ± 0.69	1.25 ± 0.57
This work	Interannual	ERBE 1985–1998 except 1991–1993	HadCRUT3	2.78 ± 0.80	−2.66 ± 1.62	0.04 ± 1.03
This work	Interannual	CERES 2000–2005 (60°S–60°N)	HadCRUT3	2.13 ± 0.88, 3.3 ± 1.3	−1.10 ± 0.79, −2.7 ± 1.6	1.03 ± 0.58, 1.8 ± 0.9
This work	Interannual	CERES 2000–2005 (global)	HadCRUT3	1.64 ± 0.84, 3.0 ± 1.4	−0.95 ± 0.81, −2.9 ± 2.0	0.69 ± 0.78, 3.0 ± 2.5
Tsushima et al. [2005]	Seasonal cycle	1985–1990	NCEP	2.06 ± 0.17	−1.07 ± 0.07	0.98 ± 0.20
Forster and Gregory [2006]	Interannual	ERBE 1985–1996 except 1993	GISS	3.8 ± 0.8	−1.6 ± 1.1	2.3 ± 0.43
Forster and Gregory [2006]	Seasonal	ERBE 1985–1996	GISS	2.7 ± 1.2	−1.3 ± 1.6	1.5 ± 0.7
Forster and Taylor [2006]	Average of 20 global climate models	~220-year model runs	Each model	2.3 ± 0.37	−0.89 ± 0.53	1.42 ± 0.32
Soden and Held [2006]	Average of 12 global climate models	~100-year model runs	Each model			1.28 ± 0.29

[a]Here λ is in W m^{-2} K^{-1}.
[b]The second line of values is the orthogonal distance regression.

of global temperatures suggest that the surface ocean portion of the Earth's climate response has a time constant of about 8–12 years [*Scafetta*, 2008; *Schwartz*, 2008]. In Figure 2, much of the temperature variation is on time scales much shorter than 8 years. Thus, it is likely that temperatures changes resulting from the radiation budget are damped and the main direction is temperature changing outgoing radiation. This favors temperature as the independent variable. For comparison, orthogonal distance regressions that treat neither variable as causal and with the same relative errors are also shown in Figure 2 and Table 1. The shortwave and total residuals in Figure 2 are not random but are dominated by a semiannual cycle. Removing this semiannual cycle brings the orthogonal regression slopes much closer to the ordinary regression slopes, which do not perceptibly change.

[21] In order to examine only interannual changes, we have also performed regressions using only temperature anomalies from the annual mean. Because of data gaps and other details the methodology is more complicated and the results for both CERES and ERBE are presented in Appendix A. The results are consistent with Figure 2 but with larger statistical errors.

[22] Figure 3 and Table 1 show the slopes derived from our methods compared to some literature results. As can be seen in Figure 2, the ERBE and CERES data yield very similar slopes. For the CERES data, feedbacks can be compared for global coverage and 60°S–60°N. Including areas poleward of 60° makes the shortwave feedback stronger on a seasonal basis but not on an interannual basis. This supports the arguments advanced by *Tsushima et al.* [2005] about excessive shortwave feedbacks on seasonal time scales. However, the CERES seasonal and annual slopes are very similar when the polar regions are excluded so it seems that the seasonal slopes for data between 60°S and 60°N provide a good estimate of the interannual variability. For total outgoing radiation minus forcing the ordinary regression slopes for λ are 1.31 and 1.43 W m^{-2} K^{-1} for ERBE and CERES data, respectively. The ERBE and CERES interannual slopes are all less than 1.25 W m^{-2} K^{-1} whereas the seasonal slopes using orthogonal distance regression slopes are larger than 1.5 W m^{-2} K^{-1}. We adopt $\lambda = 1.25 \pm 0.5$ W m^{-2} K^{-1} as an estimate for the response of net radiation to temperature variations between the 1950 and 2004. The error estimate is spread considerably beyond the statistical errors in the fits because of the issues regarding the choice of regression.

[23] The choice of a reference temperature for ΔT in equation (1) is what provides an absolute scale for the net outgoing radiation. By convention, radiative forcings are referenced to preindustrial conditions. Because we explicitly include the forcing from large volcanic eruptions [*Robock*, 2000], to be self-consistent the reference temperature should correspond to preindustrial conditions without cooling from large eruptions. The 1950s were probably warmer than the reference condition since for several decades prior to that there were no major volcanic eruptions and some positive anthropogenic climate forcing. The late 19th century was probably cooler than our desired nonvolcanic reference condition because of Krakatoa and lingering effects of the Tambora eruption in 1815. Temperatures from 1950 to 1959 were about 0.2 K warmer than they were from 1850 to 1910 [*Brohan et al.*, 2006]. Using these periods as bounds, we choose a reference temperature 0.14 ± 0.1 K cooler than the average of 1950 to 1959, or −0.29 K on the HadCRUT3 relative temperature scale.

[24] Using our best estimate of λ, an uncertainty of ±0.1 K in the reference temperature contributes ±0.125 W m^{-2} uncertainty to total outgoing radiation using. This is much smaller than the absolute uncertainty of the ERBE or CERES instruments.

4. Time History and Aerosol Forcing

[25] The time history of the energy budget contains information in addition to the integrated quantities. A history

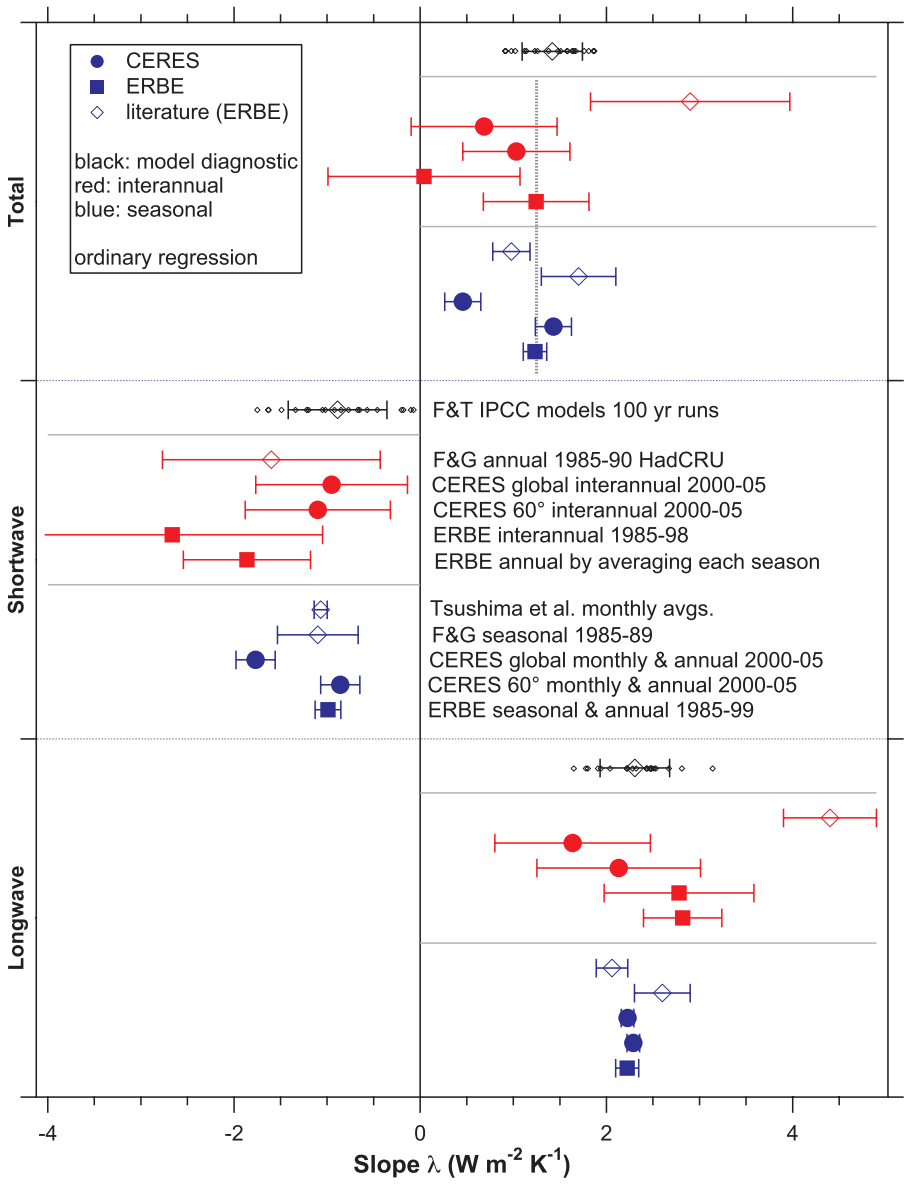

Figure 3. Summary of various calculations of λ for longwave, shortwave, and total radiation. The bottom two solid points in each category are the slopes from Figure 2. The next point up is a similar analysis for global CERES data rather than 60°S–60°N. It shows a nearly identical longwave response but a much stronger shortwave response from snow in the polar regions. The open blue points are literature values including seasonal variation [*Tsushima et al.*, 2005; *Forster and Gregory*, 2006]. The solid red points are slopes of interannual data for ERBE and CERES data (Appendix A). The open red point is a literature value for a subset of the ERBE data [*Forster and Gregory*, 2006]. The open black points are regressions of outgoing radiation minus forcing against temperature for 20 models in the IPCC archive [*Forster and Taylor*, 2006]. Values plotted here are ordinary regression; see Table 1 for the slopes of orthogonal distance regressions. The dotted vertical line in the total section is the value used in this paper.

of anthropogenic radiative forcing (excluding aerosols) and volcanic radiative forcing is shown in Figure 4a along with the radiative response of a warming Earth using $\lambda = 1.25 \pm 0.5$ W m^{-2} K^{-1}. A time history of the energy going to heat the Earth (Figure 4b) requires differentiating the heat content. The ocean heat content data are too noisy for single year differences, so successive linear fits were performed to running 8-year segments of data. Eight years is the longest period that still cleanly separates the dips due to El Chichon and Mt. Pinatubo. The error bars are the 1σ uncertainties in the slope including both the scatter and uncertainties in the ocean heat data. Some of the ocean heat errors probably are systematic over a period of a few years. For example, similar regions are probably undersampled in successive years. If so, the error bars on Figure 4b would overestimate the uncertainty in the derivative of the ocean heat content. On the other hand, the error bars would underestimate the uncertainty if most of the warming took place in poorly sampled regions

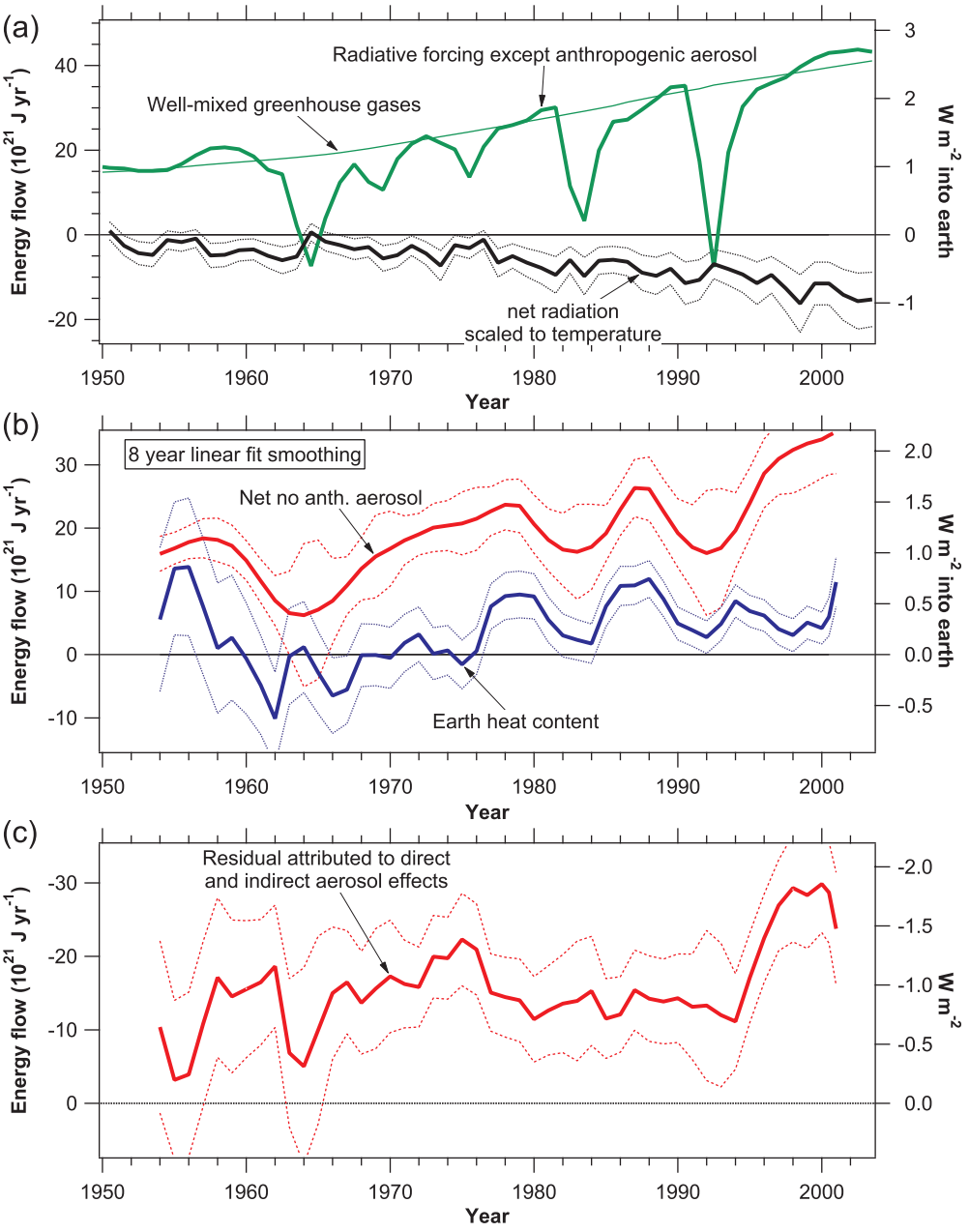

Figure 4. Time history of radiative forcings and energy budget terms. (a) Radiative forcing and the increased net radiation from a warming Earth $-\lambda\Delta T$ with $\lambda = 1.25$ W m^{-2} K^{-1}. (b) The derivative of the Earth heat content using *Domingues et al.* [2008] for the ocean. The red curve is forcing plus Earth radiative response (the sum of the green and black curves in Figure 4a) smoothed in the same manner as the heat content. There is very good agreement for the dips in 1963, 1982, and 1992 due to volcanic eruptions. (c) The remaining forcing, which is the difference between the red and blue curves in Figure 4b. Note the inverted scale, as the remaining forcing is negative. The dotted lines represent 1σ limits.

such as the Southern Ocean. For consistency, the radiative forcings were smoothed in the same manner: lines were fit to 8-year segments of integrated forcing.

[26] The difference between the smoothed forcing and the derivative of the Earth heat content represents forcings not included in the calculations to this point. The largest such forcings are expected to be the aerosol direct and indirect effects [see *Forster et al.*, 2007]. Figure 4c shows the remaining heat flow attributable mostly to aerosols. The dashed limits come from adding uncertainties in quadrature because errors in radiative forcing calculations, ocean heat content, and ERBE heat fluxes are independent of each other. Using the *Domingues et al.* [2008] ocean heat content, the average value of estimated aerosol direct and indirect radiative forcing from 1970 to 2000 is $-17 \pm 6 \times 10^{21}$ J a^{-1}, or -1.06 ± 0.4 W m^{-2} (1σ). We have conservatively set the error estimate for the 30-year average to the average error for a single year.

[27] Figure 5 compares the history of the residual forcing to some indicators of anthropogenic aerosols. The general

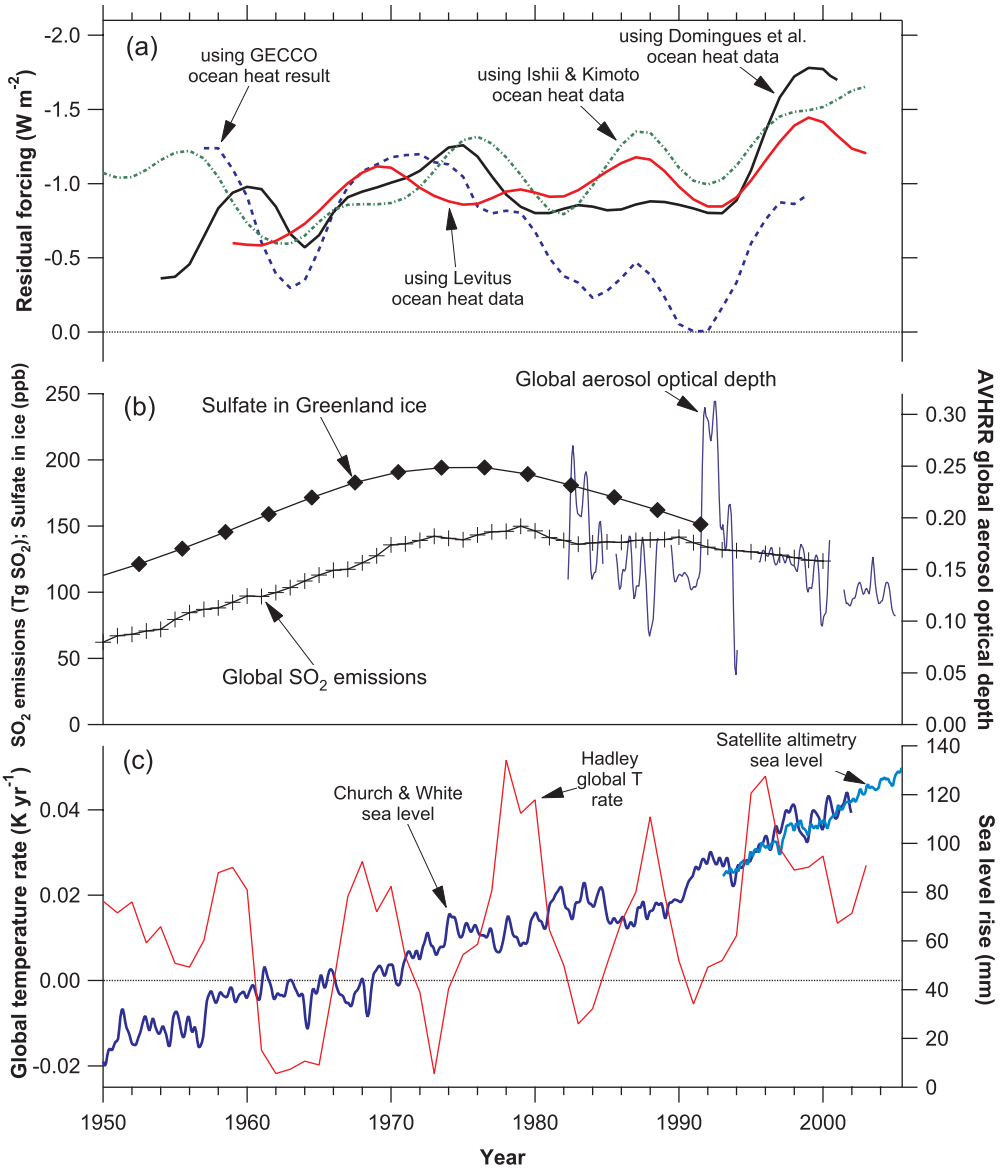

Figure 5. Residual forcing attributed to direct and indirect aerosol effects compared to several measures indicative of this forcing. (a) A slightly smoothed version of the residual in Figure 4c along with calculations using other estimates of the ocean heat content. (b) Greenland ice sulfate values are an average of three cores [*Fischer et al.*, 1998], global SO_2 emissions are from a compilation by *Smith et al.* [2004], and AVHRR aerosol optical depths are a smoothed version of *Zhao et al.* [2008]. (c) A history of sea level rise [*Church and White*, 2006] and the rate of change of global surface temperatures with an 8-year smoothing, as in Figure 2. Satellite altimetry sea levels are offset vertically to overlap the historical record.

increase from 1950 to 1970 followed by level forcing or a slight decrease into the 1980s is consistent with measures of anthropogenic forcing. Sulfate in Greenland ice [*Fischer et al.*, 1998] increased from 1950 to the early 1970s, then declined as emission controls were adopted in North America and Europe. Global sulfur dioxide emissions [*Smith et al.*, 2004] had smaller decreases after 1970 as lower emissions in North America and Europe were offset by increases elsewhere. In agreement with other recent analyses [*Alpert et al.*, 2005; *Wild et al.*, 2005], the residual forcing does not support continued "global dimming" past the early 1970s.

[28] Also shown in Figure 5 are histories of the residual forcing if other ocean heat content analyses are used in place of *Domingues et al.* [2008]. The GECCO ocean model assimilates data from a variety of sources [*Köhl and Stammer*, 2008]. It obtains a rather different time history than most of the other ocean heat analyses summarized by *Carton and Santorelli* [2008].

[29] When using the *Domingues et al.* [2008] data, there is a jump in the computed residual forcing in about 1995 (Figures 4c and 5). The other data sets have a smaller but similar change. Possible explanations include errors in the measured ocean heat uptake (due, e.g., to changing instrument types) or a temporary transport of heat to the deep

Table 2. Combined Aerosol Direct and Indirect Forcings

Source	Time Period	Ocean Heat	Greenhouse Forcings	Aerosol Forcing (W m^{-2})	2σ or 90% Confidence Limits (W m^{-2})
This work's best estimate	Preindustrial to 1970–2000	*Domingues et al.* [2008]	*Gregory and Forster* [2008]	−1.06	−0.3 to −1.9
This work	Preindustrial to 1970–2000	*Domingues et al.* [2008]	GISS	−1.21	−0.4 to −2.0
This work	Preindustrial to 1970–2000	*Levitus et al.* [2009]	*Gregory and Forster* [2008]	−1.04	−0.3 to −1.7
This work	Preindustrial to 1970–2000	*Ishii and Kimoto* [2009]	*Gregory and Forster* [2008]	−1.15	Not calculated
This work	Preindustrial to 1970–2000	*Köhl and Stammer* [2008]	*Gregory and Forster* [2008]	−0.62	Not calculated
IPCC AR4 chapter 2 (direct and cloud albedo forcings)[a]	Preindustrial to circa 2005	–	–	−1.2	−0.6 to −2.4 (forward estimates)
IPCC AR4 chapter 7 (total aerosol forcings)[b]	Preindustrial to circa 2005	–	–	−1.2	−0.2 to −2.3 (full model range)
IPCC AR4 chapter 9 (total aerosol forcings)[c]	Preindustrial to circa 2005	–	–		−0.1 to −1.7 (inverse estimates)

[a] *Forster et al.* [2007].
[b] *Denman et al.* [2007].
[c] *Hegerl et al.* [2007].

ocean. An explanation that can be largely excluded is a jump in aerosol forcing from increasing Asian emissions or other rapid changes in aerosols. A jump in aerosol forcing in the mid-1990s would show up as an increase in global albedo while the ERBE time series shows decreases rather than increases in albedo then. Trends in cloudiness are problematic because of changes in satellite viewing angles [*Evan et al.*, 2007], but uncorrected International Satellite Cloud Climatology Project (ISCCP) data given by Evan *et al.* also show a also decrease rather than an increase in the late 1990s. Finally, except for Mt. Pinatubo, the global average aerosol optical depth was constant or slightly decreasing from 1985 to 2000 (Figure 5b) [*Wild et al.*, 2005; *Mishchenko et al.*, 2007; *Zhao et al.*, 2008]. It is unlikely that there could be a large increase in global aerosol radiative forcing at a time when the average optical depth was constant or declining. Taken together, these lines of evidence suggest that the increase in aerosol forcing through the 1960s and stabilization in the 1970s are real but the apparent jump in the late 1990s is questionable.

[30] One possible explanation for the change in the residual around 1996 is an underestimate of ocean heat uptake. Figure 4b shows that the jump in the residual forcing can be traced to a decrease in the estimated ocean heat uptake around 1996 rather than changes in other climate forcings. Figure 5c shows no corresponding decrease in the rate of sea level rise as would be expected if the oceans had stopped warming. Figure 3 from *Domingues et al.* [2008] confirms that the computed sea level rise is less than that observed by satellite altimetry starting in about 1996. One way to make the heat uptake and sea level rise data consistent would be a shift around 1996 from ocean warming to an increase in glacial melting or other sources of sea level rise that require less energy than thermal expansion. However, rather than such a shift in physical mechanisms, a simple possibility is that errors in the heat content data cause an underestimate of the thermal expansion contribution to sea level rise as well as the apparent jump in forcing in the late 1990s. Ocean heat uptake based on Argo float data also disagrees with sea level rise after 2003, with no statement on which is correct [*Willis et al.*, 2008]. The German contribution to Estimating the Circulation and Climate of the Ocean (GECCO) ocean assimilation model suggests that since the mid-1990s more heat may have been going into the deep ocean [*Köhl and Stammer*, 2008].

5. Discussion

[31] The magnitude of the residual forcing agrees well within combined uncertainties with the IPCC AR4 best estimates of −0.5 and −0.7 W m^{-2} for the direct and cloud albedo indirect aerosol effects in 2005, respectively [*Forster et al.*, 2007]. It also fits the IPCC AR4 total aerosol climate forcing estimate including lifetime and semidirect effects of roughly 1.2 W m^{-2} [*Denman et al.*, 2007]. However, the residual derived here excludes at the 2σ level large estimates of the aerosol indirect effect that would lead to combined aerosol forcings more negative than about −1.9 W m^{-2}. This narrows the uncertainty range compared to the IPCC AR4 estimates (Table 2). Former discrepancies between top-down and bottom-up estimates of aerosol forcing [*Anderson et al.*, 2003] are not supported by our analysis.

[32] There are two somewhat different ways of using our results to constrain climate sensitivity. The first way is to combine the upper limit on aerosol forcing, which is not very sensitive to λ, with previous model results. To be consistent with recent temperature history, global climate models with very high climate sensitivities must have a large ocean heat uptake or a small net forcing. Such a small net forcing arises if aerosol indirect effects are so large that they nearly cancel greenhouse gas forcing [*Foster et al.*, 2008; *Knutti*, 2008]. The limit derived here on combined aerosol forcings of −1.9 W m^{-2} would constrain climate sensitivity in the work of *Andreae et al.* [2005] to less than about 10°C for doubled CO_2, a rather weak upper bound.

[33] A second way of constraining climate sensitivity is to argue directly from values of λ. Again, the data provide only a weak upper bound on climate sensitivity. Although we repeat that values of λ derived over a period of several years are not necessarily the same as the long-term inverse climate sensitivity, the nearly 15-year ERBE record is long enough for at least some slower feedback processes such as Arctic sea ice to begin to operate. Depending on how one treats data gaps, the best fit increase in interannual outgoing

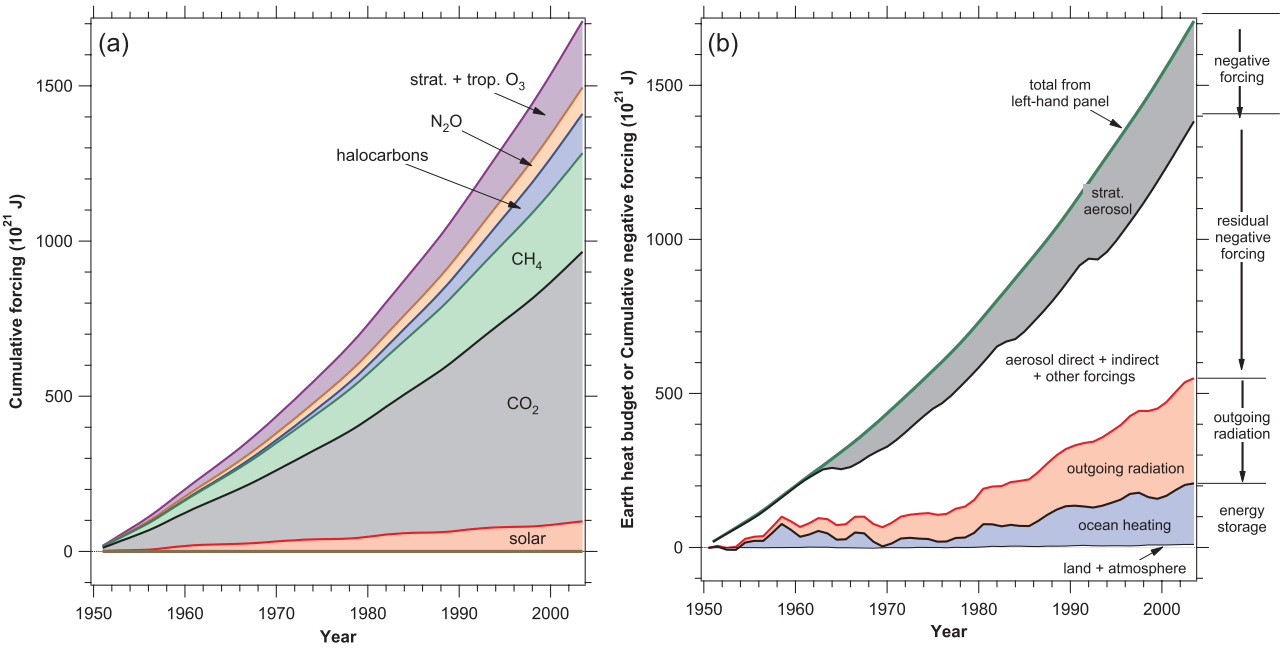

Figure 6. Cumulative energy budget for the Earth since 1950. (a) Mostly positive and mostly long-lived forcing agents from 1950 through 2004. (b) The positive forcings have been balanced by stratospheric aerosols, direct and indirect aerosol forcing, increased outgoing radiation from a warming Earth and the amount remaining to heat the Earth. The aerosol direct and indirect effects portion is a residual after computing all other terms.

radiation was between 0.04 and 1.25 W m^{-2} K^{-1} (Figure 2 and Table 1). This does not exclude the inverse climate sensitivity of 0.37 W m^{-2} K^{-1} for a 10°C warming for doubled CO_2.

[34] The shortwave satellite data may place a lower bound on climate sensitivity. Model sensitivities to seasonal changes in snow cover and long-term snow and ice albedo feedback are highly correlated [*Hall and Qu*, 2006]. Two of the AR4 models have shortwave λ values smaller (less negative) than -0.11 W m^{-2} K^{-1}, outside the error limits of both the ERBE and CERES results for either seasonal or interannual regressions (Figure 3; model λ values from *Forster and Taylor* [2006]). These models (PCM and FGOALS) have the lowest and third lowest climate sensitivities of all the models in the IPCC AR4 at 2.1°C and 2.3°C for CO_2 doubling, respectively [*Randall et al.*, 2007], suggesting that it may be difficult to reconcile doubled CO_2 climate sensitivities as low as 2°C with the ERBE and CERES results.

[35] Overall, the constraints on climate sensitivity from this observationally based analysis are similar to those from model-based analyses: the recent climate record provides stronger constraints at the low end of the climate sensitivity than at the high end [*Foster et al.*, 2008; *Knutti and Hegerl*, 2008]. *Tomassini et al.* [2007] use a formal statistical analysis to show the asymmetric distribution of sensitivity estimates. It is interesting that their statistical analysis identifies ocean heat content, a quantity that is related to conservation of energy, as an important constraint.

[36] The consistency of the residual with independent, bottom-up estimates of aerosol direct and indirect effects means that it is very unlikely that there are any comparably large climate forcings not currently being considered. Any other large, unknown forcings would not only have to nearly cancel each other in today's conditions but would have to be consistent with the time history of aerosol forcing, as supported by observations of sulfate in Greenland ice cores (see Figure 5). This finding supports the idea that the small warming in the 1960s and 1970s was likely due to increased aerosol then.

[37] Figure 6 shows a best estimate of the energy balance of the Earth since 1950. Figure 6a shows the sum of mostly positive, long-term climate forcings. Figure 6b shows how these forcings have been balanced to conserve energy by short-term negative forcings, heat uptake, and increased outgoing radiation.

[38] A striking result of the Earth energy budget analysis presented here is the small fraction of greenhouse gas forcing that has gone into heating the Earth. Since 1950, only about 10 ± 7% of the forcing by greenhouse gases and solar radiation has gone into heating the Earth, primarily the oceans. About 20 ± 9% has been balanced by increased outgoing radiation. About 20% of the forcing by greenhouse gases and solar radiation has been offset by volcanic aerosols. The remainder, about 50%, has been balanced by the direct and indirect effects of anthropogenic aerosols. Many global climate models roughly reproduce the ratio whereby radiative response accounts for about twice as much energy as ocean heat uptake [*Gregory and Forster*, 2008].

[39] The heat capacities of the atmosphere, land, and top few meters of the ocean are small compared to both the ocean to 700 m depth and the energy from years of integrated radiative forcings. Small changes in heat transfer into the ocean, cloudiness, or other terms can create significant changes in surface temperature. Therefore, from

an energy conservation point of view there is no inconsistency in surface warming proceeding unevenly. Oscillations in the rate of surface warming are apparent in Figure 5c. Some, but not all, maxima in the rate of temperature increase come after the dips due to major volcanic eruptions. For example, the temperature increased very rapidly in 1995 to 1996. This is not surprising from an energy budget point of view. The stratospheric aerosol had declined nearly to background levels, yet surface temperatures were still reduced because of the cooling after the eruption of Mt. Pinatubo. That means that there was less outgoing radiation, giving an enhanced net flow of energy to the Earth.

[40] Questions have been raised in the popular media about the reduced rate of warming since 1998 (e.g., http://transcripts.cnn.com/TRANSCRIPTS/0901/13/ldt.01.html; http://www.realclimate.org/index.php/archives/2009/01/cnn-is-spun-right-round-baby-right-round/langswitch_lang/in#more-640). Figure 5 shows that the recent change in the atmospheric warming rate is not unusual compared to the decadal variability in the rate of warming over the past 50 years [*Easterling and Wehner*, 2009]. Further, unless there have been surprisingly large contributions other than thermal expansion to sea level since 1998 the continued rise (Figure 5c) suggests that a significant amount of energy has gone into the oceans rather than warming the surface. Changes in observing systems make it difficult to more fully compare the energy budget before and after 1998. The ERBE data on the ERBS satellite end in 1999 and the CERES data start in 2000. At about the same time there was also a significant shift in ocean temperature measurements from XBTs to profiles from floats [*AchutaRao et al.*, 2007; *Gouretski and Koltermann*, 2007]. Nevertheless, the observations of sea level since 1998 show that interpretation of increasing or decreasing rates of warming of the Earth requires consideration of both ocean and atmosphere.

[41] The small fraction of retained energy is a reminder of how quickly radiative imbalances can heat the Earth. It is energetically possible for surface temperature to increase or sea levels to rise much more rapidly than they have in the recent past. In the long run, positive radiative forcings must be balanced by increases in the outgoing energy from Earth to space [*Hansen et al.*, 2005]. That process is already making a significant contribution to the Earth's energy balance.

Appendix A: Estimates of λ From Surface Temperatures and Satellite Radiance Data

[42] Following equation (1), $-\lambda$ is the slope of *N-F* versus ΔT. Note that since outgoing radiations are negative, a positive forcing makes the magnitude of *N-F* larger. The temporal changes in the forcing *F* from greenhouse gases and volcanic aerosols are included in the regressions. Possible year-to-year changes in aerosol forcing could affect the fits but are small, according to the AVHRR record of aerosol optical thickness (Figure 5c), which covers both the ERBE and CERES periods. After removing an estimate of the stratospheric aerosol optical thickness consistent with the GISS stratospheric forcing, the recent linear trend is -0.0002 optical depth units per year (data from *Zhao et al.* [2008]).

[43] Small differences in forcing of up to about ± 0.034 W m^{-2} caused by the seasonal cycle in CO_2 were removed from all regressions using average departures of monthly global CO_2 from the long-term trend between 1984 and 1999 (NOAA Global Monitoring Division http://www.esrl.noaa.gov/gmd/dv/ftpdata.html). A similar cycle of up to ± 0.16 W m^{-2} caused by seasonal forcing of aerosol optical thickness was removed from all regressions using monthly average aerosol optical thickness in nonvolcanic years (Figure 5c) [*Zhao et al.*, 2008]. Removing the seasonal cycles in forcing slightly improved the fits. For example, the r^2 of the CERES shortwave data improved from 0.40 to 0.45. All slopes changed by amounts much smaller than the statistical error limits. The residuals from fits against temperature have a seasonal cycle. For example, the standard deviation of the global total outgoing radiation residuals from a fit against temperature is 1.92 W m^{-2} but is only 0.61 W m^{-2} after annual and semiannual cycles are removed. The maximum absolute value of the correlation between NCEP 1000 mbar temperature and both longwave and shortwave CERES data is at zero lag. Total outgoing radiation has the largest absolute correlation at either zero or two month lag, depending on whether 60°S–60°N or global data are considered.

[44] Figure A1 shows regressions of surface temperatures and satellite radiative flux data using only interannual variations. Compared to Figure 2, an advantage is that these regressions over 15 years (ERBE) or 5.75 years (CERES) are good surrogate for what we use λ for in this paper, interannual variations over 55 years. The disadvantage is that interannual changes in temperature are small, leading to more uncertainty in the slope. Interannual changes also rely more on the long-term stability of the ERBE and CERES instruments. For example, there may have been offsets introduced into the ERBE data by the power down in 1993 [*Trenberth*, 2002]. Multiple lines of evidence show that these affect the data by less than 0.5 W m^{-2} [*Wielicki et al.*, 2002]. However, a step change of 0.5 W m^{-2} in 1993 would change the slope in Figure A1a by about 1 W m^{-2} K^{-1}, showing the stringent requirements on long-term stability if annual averages are used.

[45] Using a comparison to SeaWiFS data [*Loeb et al.*, 2007], the 1σ precision for shortwave CERES data on Terra can be estimated as 0.2 W m^{-2} for monthly averages. The CERES longwave precision is estimated to be 0.36 W m^{-2} (N. Loeb, private communication, 2009), although the scatter in the residuals in fits such as Figure 2 is considerably smaller than this.

[46] For interannual regressions we use the HadCRUT3 temperature record (http://www.cru.uea.ac.uk/cru/data/temperature/ [*Brohan et al.*, 2006]) instead of the NCEP record used in Figure 2. The HadCRUT3 temperature record is very well suited for interannual variations. We use the NCEP record for Figure 2 because the HadCRUT3 data are deseasonalized at the station level and therefore cannot easily include the seasonal variation of global temperature (P. Brohan, personal communication, 2008). A comparison of the HadCRUT3 and NCEP records for the ERBE and CERES periods is shown in Figure S1.[1] Monthly average temperatures were interpolated onto the ERBE periods over the 60°S

[1] Auxiliary materials are available in the HTML. doi:10.1029/2009JD012105.

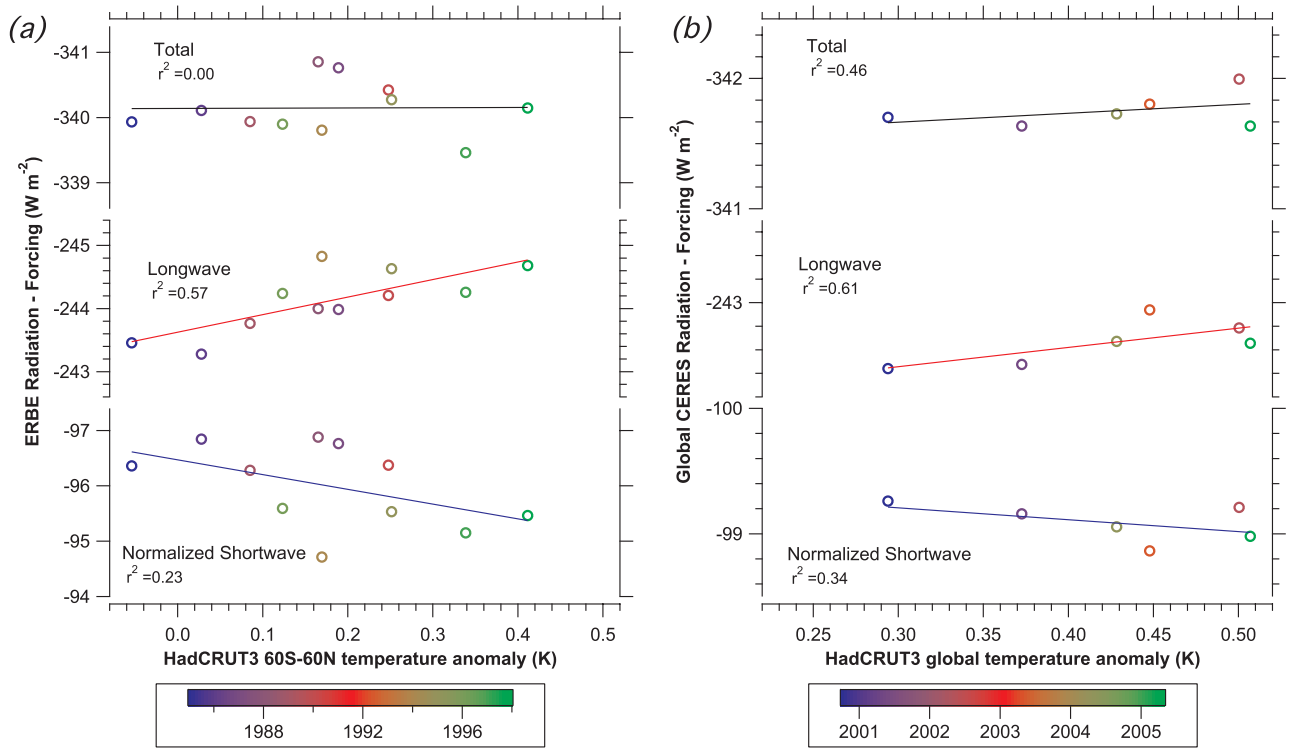

Figure A1. Regressions of annual averages of (a) ERBE and (b) CERES outgoing radiation. Shown are ERBE wide field of view data that cover about 60°S–60°N and global coverage from CERES.

to 60°N latitude range covered by the ERBE wide field of view sensor or the appropriate latitude range for CERES.

[47] There are gaps in the ERBE data in late 1993, early 1998, and early 1999. It is difficult to use partial years because the results become sensitive to how seasonal variations are removed. In addition, the rapidly changing radiative forcing after the eruption of Mt. Pinatubo in 1991 makes the data difficult to interpret through about 1993. One approach is to restrict the analysis to complete data before 1991, but that fails to utilize information from the warm years in the later 1990s. The data in Figure A1 cover complete years from 1985 through 1990 and 1994 through 1997. In addition, a composite "1998" was created using data from 1997 and 1999 to fill gaps in the 1998 record

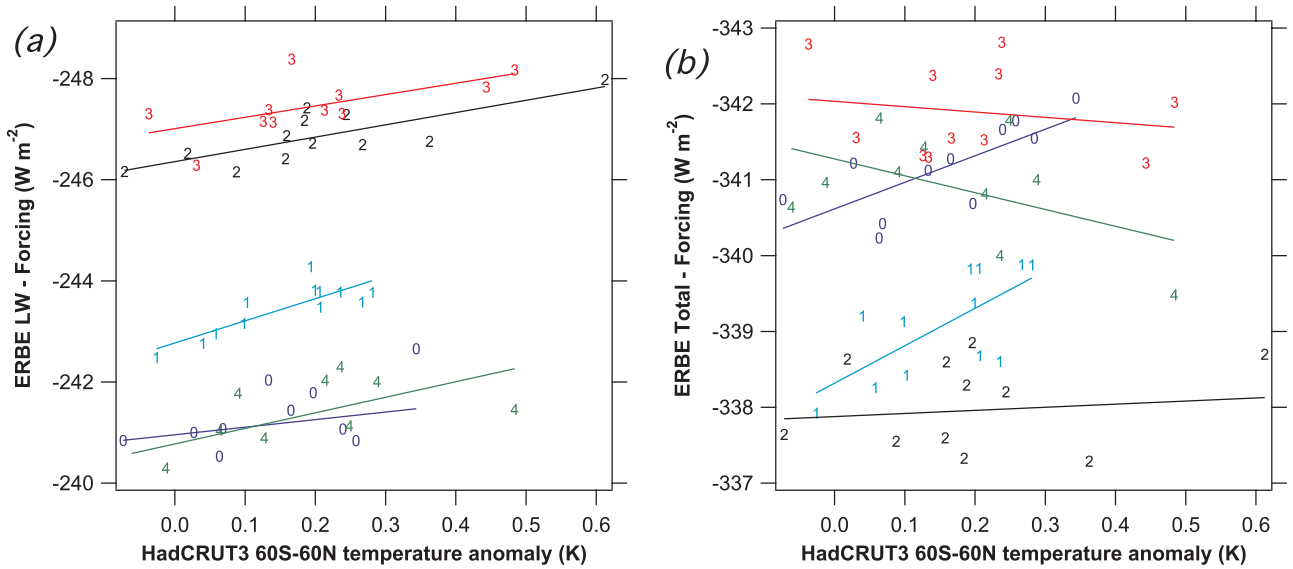

Figure A2. Separate regressions for each 72-day season of ERBE outgoing radiation modified by changes in radiative forcing for (a) longwave radiation and (b) the total outgoing radiation. For example, the points with "0" markers represent data for the first 72 days of each year. The five slopes can then be averaged to give an annual average slope.

along with the temperature anomalies corresponding to those intervals rather than calendar 1998.

[48] As an alternative to annual averages, we have also performed separate regressions for each 72-day ERBE season and then averaged the slopes from the different seasons to obtain an annual average (Figure A2). These regressions make use of all the ERBE data except for the 2 years following the eruption of Mt. Pinatubo. A disadvantage is that different seasons contain different years. The slopes are different than the slopes derived from simple annual averages but are within the overlapping error bars, as they should be when including or excluding a few points from a data set.

[49] The CERES data cover March 2000 though October 2005. We obtain 6 annual points by using March 2000 to February 2001 as the first point, then November 2000 to October 2001 and so on. The error limits in Table 1 are expanded slightly from the fitted errors to account for the first two points not being completely independent of each other.

[50] Finally, regressions analogous to Figure 2 were repeated using NCEP temperatures from other levels besides 1000 mbar. This is of interest because much of the outgoing longwave radiation originates from levels above the surface. The slope of longwave radiation with temperature was larger at 850 mbar (2.46 W m^{-2} K^{-1}) than at the surface (2.21 W m^{-2} K^{-1}), consistent with there being less water vapor feedback at the higher altitude and hence a value closer to the blackbody slope.

[51] **Acknowledgments.** This work was supported by NOAA base and climate change funding. T. Wong is supported by the NASA Science Mission Directorate through the CERES Project at the NASA Langley Research Center. We thank a number of people for digital versions of published data, including C. M. Domingues, J. A. Church, M. Ishii, and A. Koehl for ocean heat content; J. M. Gregory for radiative forcing; and T. Zhao for AVHRR optical depth. Sea level files were obtained from the CSIRO web site, stratospheric forcing history was obtained from the GISS web site, and global temperature history was obtained from the Hadley Centre web site. The CERES data are from the NASA Langley Atmospheric Science Data Center. *Levitus et al.* [2009] data are available from the NOAA Oceanographic Data Center (ftp://ftp.nodc.noaa.gov/pub/data.nodc/woa/DATA_ANALYSIS/3M_HEAT_CONTENT/DATA/basin/yearly/h22-w0-700m.dat). NCEP Reanalysis data were provided by the NOAA ESRL Physical Sciences Division from their web site (http://www.cdc.noaa.gov/).

References

AchutaRao, K. M., M. Ishii, B. D. Santer, P. J. Gleckler, K. E. Taylor, T. P. Barnett, D. W. Pierce, R. J. Stouffer, and T. M. L. Wigley (2007), Simulated and observed variability in ocean temperature and heat content, *Proc. Natl. Acad. Sci. U. S. A.*, *104*, 10,768–10,773, doi:10.1073/pnas.0611375104.

Alpert, P., P. Kishcha, Y. J. Kaufman, and R. Schwarzbard (2005), Global dimming or local dimming?: Effect of urbanization on sunlight availability, *Geophys. Res. Lett.*, *32*, L17802, doi:10.1029/2005GL023320.

Anderson, T. L., R. J. Charlson, S. E. Schwartz, R. Knutti, O. Boucher, H. Rodhe, and J. Heintzenberg (2003), Climate forcing by aerosols—A hazy picture, *Science*, *300*, 1103–1104, doi:10.1126/science.1084777.

Andreae, M. O., C. D. Jones, and P. M. Cox (2005), Strong present-day aerosol cooling implies a hot future, *Nature*, *435*, 1187–1190, doi:10.1038/nature03671.

Andrews, T., and P. M. Forster (2008), CO_2 forcing induces semi-direct effects with consequences for climate feedback interpretations, *Geophys. Res. Lett.*, *35*, L04802, doi:10.1029/2007GL032273.

Barnett, T. P., D. W. Pierce, K. M. AchutaRao, P. J. Gleckler, B. D. Santer, J. M. Gregory, and W. M. Washington (2005), Penetration of human-induced warming into the world's oceans, *Science*, *309*, 284–287, doi:10.1126/science.1112418.

Bindoff, N. L., et al. (2007), Observations: Oceanic climate change and sea level, in *Climate Change 2007: The Physical Science Basis. Contribution of Working Group I to the Fourth Assessment Report of the Intergovernmental Panel on Climate Change*, edited by S. Solomon et al., pp. 385–432, Cambridge Univ. Press, Cambridge, U. K.

Brohan, P., J. J. Kennedy, I. Harris, S. F. B. Tett, and P. D. Jones (2006), Uncertainty estimates in regional and global observed temperature changes: A new dataset from 1850, *J. Geophys. Res.*, *111*, D12106, doi:10.1029/2005JD006548.

Carton, J. A., and A. Santorelli (2008), Global decadal upper-ocean heat content as viewed in nine analyses, *J. Clim.*, *21*, 6015–6035, doi:10.1175/2008JCLI2489.1.

Church, J. A., and N. J. White (2006), A 20th century acceleration in global sea level rise, *Geophys. Res. Lett.*, *33*, L01602, doi:10.1029/2005GL024826.

Church, J. A., N. J. White, and J. M. Arblaster (2005), Significant decadal-scale impact of volcanic eruptions on sea level and ocean heat content, *Nature*, *438*, 74–77, doi:10.1038/nature04237.

Collins, W. D., et al. (2006), Radiative forcing by well-mixed greenhouse gases: Estimates from climate models in the Intergovernmental Panel on Climate Change (IPCC) Fourth Assessment Report (QR4), *J. Geophys. Res.*, *111*, D14317, doi:10.1029/2005JD006713.

Delworth, T. L., V. Ramaswamy, and G. L. Stenchikov (2005), The impact of aerosols on simulated ocean temperature and heat content in the 20th century, *Geophys. Res. Lett.*, *32*, L24709, doi:10.1029/2005GL024457.

Denman, K. L., et al. (2007), Couplings between changes in the climate system and biogeochemistry, in *Climate Change 2007: The Physical Science Basis. Contribution of Working Group I to the Fourth Assessment Report of the Intergovernmental Panel on Climate Change*, edited by S. Solomon, pp. 499–587, Cambridge Univ. Press, Cambridge, U. K.

Domingues, C. M., J. A. Church, N. J. White, P. J. Gleckler, S. E. Wijffels, P. M. Barker, and J. E. Dunn (2008), Improved estimates of upper-ocean warming and multi-decadal sea-level rise, *Nature*, *453*, 1090–1093, doi:10.1038/nature07080.

Easterling, D. R., and M. F. Wehner (2009), Is the climate warming or cooling?, *Geophys. Res. Lett.*, *36*, L08706, doi:10.1029/2009GL037810.

Evan, A. T., A. K. Heidinger, and D. J. Vimont (2007), Arguments against a physical long-term trend in global ISCCP cloud amounts, *Geophys. Res. Lett.*, *34*, L04701, doi:10.1029/2006GL028083.

Fasullo, J. T., and K. E. Trenberth (2008), The annual cycle of the energy budget. Part I: Global mean and land–ccean exchanges, *J. Clim.*, *21*, 2297–2312, doi:10.1175/2007JCLI1935.1.

Fischer, H., D. Wagenbach, and J. Kipfstuhl (1998), Sulphate and nitrate firn concentrations on the Greenland ice sheet: 2. Temporal anthropogenic deposition changes, *J. Geophys. Res.*, *103*, 21,935–21,942, doi:10.1029/98JD01886.

Forster, P., et al. (2007), Changes in atmospheric constituents and in radiative forcing, in *Climate Change 2007: The Physical Science Basis. Contribution of Working Group I to the Fourth Assessment Report of the Intergovernmental Panel on Climate Change*, edited by S. Solomon, pp. 129–234, Cambridge Univ. Press, Cambridge, U. K.

Forster, P. M. F., and J. M. Gregory (2006), The climate sensitivity and its components diagnosed from Earth Radiation Budget Data, *J. Clim.*, *19*, 39–52, doi:10.1175/JCLI3611.1.

Forster, P. M. F., and K. E. Taylor (2006), Climate forcings and climate sensitivities diagnosed from coupled climate model integrations, *J. Clim.*, *19*, 6181–6194, doi:10.1175/JCLI3974.1.

Foster, G., J. D. Amman, G. A. Schmidt, and M. E. Mann (2008), Comment on "Heat capacity, time constant, and sensitivity of Earth's climate system" by S. E. Schwartz, *J. Geophys. Res.*, *113*, D15102, doi:10.1029/2007JD009373.

Gouretski, V., and K. P. Koltermann (2007), How much is the ocean really warming?, *Geophys. Res. Lett.*, *34*, L01610, doi:10.1029/2006GL027834.

Gregory, J. M. (2000), Vertical heat transports in the ocean and their effect on time-dependent climate change, *Clim. Dyn.*, *16*, 501–515, doi:10.1007/s003820000059.

Gregory, J. M., and P. M. Forster (2008), Transient climate response estimated from radiative forcing and observed temperature change, *J. Geophys. Res.*, *113*, D23105, doi:10.1029/2008JD010405.

Gregory, J. M., R. J. Stougger, S. C. B. Raper, P. A. Stott, and N. A. Rayner (2002), An observationally based estimate of the climate sensitivity, *J. Clim.*, *15*, 3117–3121, doi:10.1175/1520-0442(2002)015<3117:AOBEOT>2.0.CO;2.

Hall, A., and X. Qu (2006), Using the current seasonal cycle to constrain snow albedo feedback in future climate change, *Geophys. Res. Lett.*, *33*, L03502, doi:10.1029/2005GL025127.

Hansen, J., et al. (2005), Earth's energy imbalance: Confirmation and implications, *Science*, *308*, 1431–1435, doi:10.1126/science.1110252.

Hegerl, G. C., F. W. Zwiers, P. Braconnot, N. P. Gillett, Y. Luo, J. A. Marengo Orsini, N. Nicholls, J. E. Penner, and P. A. Stott (2007), Understanding and Attributing Climate Change, in *Climate Change 2007: The Physical Science Basis. Contribution of Working Group I to the Fourth Assessment Report of the Intergovernmental Panel on Climate Change*,

edited by S. Solomon et al., pp. 663–745, Cambridge Univ. Press, Cambridge, U. K.

Ishii, M., and M. Kimoto (2009), Reevaluation of historical ocean heat content variations with time-varying XBT and MBT depth bias corrections, *J. Oceanogr.*, *65*, 287–299.

Knutti, R. (2008), Why are climate models reproducing the observed global surface warming so well?, *Geophys. Res. Lett.*, *35*, L18704, doi:10.1029/2008GL034932.

Knutti, R., and G. C. Hegerl (2008), The equilibrium sensitivity of the Earth's temperature to radiation changes, *Nat. Geosci*, *1*, 735–743, doi:10.1038/ngeo337.

Knutti, R., T. F. Stocker, F. Joos, and G.-K. Plattner (2002), Constraints on radiative forcing and future climate change from observations and climate model ensembles, *Nature*, *416*, 719–723, doi:10.1038/416719a.

Knutti, R., S. Krähenmann, D. J. Frame, and M. R. Allen (2008), Comment on "Heat capacity, time constant, and sensitivity of Earth's climate system" by S. E. Schwartz, *J. Geophys. Res.*, *113*, D15103, doi:10.1029/2007JD009473.

Köhl, A., and D. Stammer (2008), Decadal sea level changes in the 50-year GECCO ocean synthesis, *J. Clim.*, *21*, 1876–1889, doi:10.1175/2007JCLI2081.1.

Köhl, A., D. Stammer, and B. Cornuelle (2007), Interannual to decadal changes in the ECCO global synthesis, *J. Phys. Oceanogr.*, *37*, 313–337, doi:10.1175/JPO3014.1.

Lacis, A., J. Hansen, and M. Sato (1992), Climate forcing by stratospheric aerosols, *Geophys. Res. Lett.*, *19*, 1607–1610, doi:10.1029/92GL01620.

Levitus, S., J. I. Antonov, J. Wang, T. L. Delworth, K. W. Dixon, and A. J. Broccoli (2001), Anthropogenic warming of Earth's climate system, *Science*, *292*, 267–270, doi:10.1126/science.1058154.

Levitus, S., J. Antonov, and T. Boyer (2005), Warming of the world ocean, 1955–2003, *Geophys. Res. Lett.*, *32*, L02604, doi:10.1029/2004GL021592.

Levitus, S., J. I. Antonov, T. P. Boyer, R. A. Locarnini, H. E. Garcia, and A. V. Mishonov (2009), Global ocean heat content 1955–2008 in light of recently revealed instrumentation problems, *Geophys. Res. Lett.*, *36*, L07608, doi:10.1029/2008GL037155.

Loeb, N. G., B. A. Wielicki, W. Su, K. Loukachine, W. Sun, T. Wong, K. J. Priestley, G. Matthews, W. F. Miller, and R. Davies (2007), Multi-instrument comparison of top-of-atmosphere reflected solar radiation, *J. Clim.*, *20*, 575–591, doi:10.1175/JCLI4018.1.

Loeb, N. G., B. A. Wielicki, D. R. Doelling, G. L. Smith, D. F. Keyes, S. Kato, N. Manalo-Smith, and T. Wong (2009), Towards optimal closure of the Earth's top-of-atmosphere radiation budget, *J. Clim.*, *22*, 748–766, doi:10.1175/2008JCLI2637.1.

Mishchenko, M. I., I. V. Geogdzhayev, W. B. Rossow, B. Cairns, B. E. Carlson, A. A. Lacis, L. Liu, and L. D. Travis (2007), Long-term satellite record reveals likely recent aerosol trend, *Science*, *315*, 1543, doi:10.1126/science.1136709.

Myhre, G., A. Myhre, and F. Stordal (2001), Historical evolution of radiative forcing of climate, *Atmos. Environ.*, *35*, 2361–2373, doi:10.1016/S1352-2310(00)00531-8.

Randall, D. A., et al. (2007), Climate models and their evaluation, in *Climate Change 2007: The Physical Science Basis. Contribution of Working Group I to the Fourth Assessment Report of the Intergovernmental Panel on Climate Change*, edited by S. Solomon, pp. 589–662, Cambridge Univ. Press, Cambridge, U. K.

Robock, A. (2000), Volcanic eruptions and climate, *Rev. Geophys.*, *38*, 191–219, doi:10.1029/1998RG000054.

Scafetta, N. (2008), Comment on "Heat capacity, time constant, and sensitivity of Earth's climate system" by S. E. Schwarz, *J. Geophys. Res.*, *113*, D15104, doi:10.1029/2007JD009586.

Schwartz, S. (2008), Reply to comments by G. Foster et al., R. Knutti et al., and N. Scafetta on "Heat capacity, time constant, and sensitivity of Earth's climate system" by S. E. Schwarz, *J. Geophys. Res.*, *113*, D15105, doi:10.1029/2008JD009872.

Smith, S. J., E. Conception, R. Andres, and J. Lurz (2004), Historical sulfur dioxide emissions 1850–2000: Methods and results, *Res. Rep. PNNL-14537*, Pac. Northwest Natl. Lab., Richland, Wash.

Soden, B. J., and I. M. Held (2006), An assessment of climate feedbacks in coupled ocean-atmosphere models, *J. Clim.*, *19*, 3354–3360, doi:10.1175/JCLI3799.1.

Stott, P. A., C. Huntingford, C. D. Jones, and J. A. Kettleborough (2008), Observed climate change constrains the likelihood of extreme future global warming, *Tellus Ser. B*, *60*, 76–81.

Stouffer, R. J. (2004), Time scales of climate response, *J. Clim.*, *17*, 209–217, doi:10.1175/1520-0442(2004)017<0209:TSOCR>2.0.CO;2.

Tomassini, L., P. Reichert, R. Knutti, T. F. Stocker, and M. E. Borsuk (2007), Robust Beyesian uncertainty analysis of climate system properties using Markov Chain Monte Carlo methods, *J. Clim.*, *20*, 1239–1254, doi:10.1175/JCLI4064.1.

Trenberth, K. E. (2002), Technical comment: Changes in tropical clouds and radiation, *Science*, *296*, 2095, doi:10.1126/science.296.5576.2095a.

Trenberth, K. E., and D. P. Stepaniak (2004), The flow of energy through the Earth's climate system, *Q. J. R. Meteorol. Soc.*, *130*, 2677–2701, doi:10.1256/qj.04.83.

Trenberth, K. E., J. T. Fasullo, and J. Kiehl (2009), Earth's global energy budget, *Bull. Am. Meteorol. Soc.*, *90*, 311–323, doi:10.1175/2008BAMS2634.1.

Tsushima, Y., A. Abe-Ouchi, and S. Manabe (2005), Radiative damping of annual variation in global mean surface temperature: Compaison between observed and simulated feedback, *Clim. Dyn.*, *24*, 591–597, doi:10.1007/s00382-005-0002-y.

Wielicki, B. A., et al. (2002), Reply to "Changes in tropical clouds and radiation," *Science*, *296*, 2095, doi:10.1126/science.296.5576.2095a.

Wijffels, S. E., J. Willis, C. M. Domingues, P. Barker, N. J. White, A. Gronell, K. Ridgway, and J. A. Church (2008), Changing eXpendable BathyThermograph fall-rates and their impact on estimates of thermosteric sea level rise, *J. Clim.*, *21*, 5657–5672, doi:10.1175/2008JCLI2290.1.

Wild, M., H. Gilgen, A. Roesch, A. Ohmura, C. N. Long, E. G. Dutton, B. Forgan, A. Kallis, V. Russak, and A. Tsvetkov (2005), From dimming to brightening: Decadal changes in solar radiation at Earth's surface, *Science*, *308*, 847–850, doi:10.1126/science.1103215.

Willis, J. K., D. P. Chambers, and R. S. Nerem (2008), Assessing the globally averaged sea level budget on seasonal to interannual timescales, *J. Geophys. Res.*, *113*, C06015, doi:10.1029/2007JC004517.

Wong, T., B. A. Wielicki, R. B. Lee III, G. L. Smith, K. A. Bush, and J. A. Willis (2006), Reexamination of the observed decadal variability of the Earth Radiation Budget Experiment using altitude-corrected ERBE/ERBS nonscanner WFOV data, *J. Clim.*, *19*, 4028–4040, doi:10.1175/JCLI3838.1.

Zhao, T. X.-P., I. Laszlo, W. Guo, A. Heidinger, C. Cao, A. Jelenak, D. Tarpley, and J. Sullivan (2008), Study of long-term trend in aerosol optical thickness observed from operational AVHRR satellite instrument, *J. Geophys. Res.*, *113*, D07201, doi:10.1029/2007JD009061.

P. M. Forster, School of Earth and Environment, University of Leeds, Leeds LS2 9JT, UK.

D. M. Murphy, R. W. Portmann, K. H. Rosenlof, and S. Solomon, Chemical Sciences Division, Earth System Research Laboratory, NOAA, 325 Broadway, Boulder, CO 80303, USA. (daniel.m.murphy@noaa.gov)

T. Wong, NASA Langley Research Center, Mail Stop 420, Hampton, VA 23681, USA.